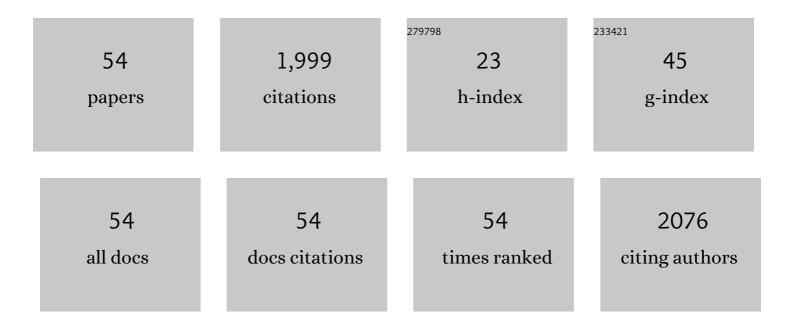
## Yoshiaki Kon

List of Publications by Year in descending order

Source: https://exaly.com/author-pdf/3748931/publications.pdf Version: 2024-02-01



#	Article	IF	CITATIONS
1	Formation of the Rock Canyon Creek carbonate-hosted REE–F–Ba deposit, British Columbia, Canada: Constraints from Mg-Sr isotopes of dolomite, calcite, and fluorite. Journal of Geochemical Exploration, 2022, , 107045.	3.2	0
2	Mineral control on the geochemistry of the Rock Canyon Creek REE-F-Ba deposit, British Columbia, Canada. Geochemistry: Exploration, Environment, Analysis, 2021, 21, geochem2020-010.	0.9	0
3	Nature and timing of anatectic event of the Hida Belt (Japan): Constraints from titanite geochemistry and U-Pb age of clinopyroxene-bearing leucogranite. Lithos, 2021, 398-399, 106256.	1.4	6
4	Experimental Study of SXES: Determination of Iron Oxidation State in Silicate Minerals. Microscopy and Microanalysis, 2020, 26, 1018-1021.	0.4	0
5	Microscopic analyses of weathered granite in ion-adsorption rare earth deposit of Jianxi Province, China. Scientific Reports, 2020, 10, 20194.	3.3	21
6	REE redistributions during granite weathering: Implications for Ce anomaly as a proxy for paleoredox states. American Mineralogist, 2020, 105, 848-859.	1.9	22
7	Sources of U and Th in groundwater of the paleobeach aquifer at Cox's Bazar, Southeast Bangladesh. Groundwater for Sustainable Development, 2020, 10, 100332.	4.6	6
8	Analytical Efficacy of a Gas Mixer and Stabilizer for Laser Ablation ICP Mass Spectrometry. ACS Omega, 2020, 5, 28073-28079.	3.5	4
9	Comparison of methods for the geochemical determination of rare earth elements: Rock Canyon Creek REE–F–Ba deposit case study, SE British Columbia, Canada. Geochemistry: Exploration, Environment, Analysis, 2019, 19, 414-430.	0.9	4
10	Zircon <scp>U–Pb</scp> dating of gabbro and diorite from the <scp>B</scp> ato pluton, northeast <scp>J</scp> apan. Island Arc, 2018, 27, e12222.	1.1	2
11	Examination of the Mass Transfer of Additive Elements in Barium Titanate Ceramics during Sintering Process by Laser Ablation ICP-MS. Analytical Sciences, 2018, 34, 739-742.	1.6	4
12	Oxidation States of Fe in Constituent Minerals of a Spinel Lherzolite Xenolith from the Tariat Depression, Mongolia: The Significance of Fe3+ in Olivine. Minerals (Basel, Switzerland), 2018, 8, 204.	2.0	12
13	Sandstone provenance and U–Pb ages of detrital zircons from Permian–Triassic forearc sediments within the Sukhothai Arc, northern Thailand: Record of volcanic-arc evolution in response to Paleo-Tethys subduction. Journal of Asian Earth Sciences, 2017, 146, 30-55.	2.3	33
14	Differential Fractionation of Rare Earth Elements in Oxidized and Reduced Granitic Rocks: Implication for Heavy Rare Earth Enriched Ion Adsorption Mineralization. Resource Geology, 2017, 67, 35-52.	0.8	15
15	Gamma radiation-induced thermoluminescence, trace element and paramagnetic defect of quartz from the Sambagawa metamorphic belt, Central Shikoku, Japan. Applied Radiation and Isotopes, 2017, 120, 30-39.	1.5	5
16	Implication of Apatite and Anhydrite for Formation of an Ironâ€Oxideâ€Apatite <b>(</b> IOA) Rare Earth Element Prospect, Benjamin River, Canada. Resource Geology, 2017, 67, 361-383.	0.8	1
17	Precipitates within olivine phenocrysts in oxidized andesitic scoria from Kasayama volcano, Hagi, Japan. Journal of Mineralogical and Petrological Sciences, 2017, 112, 116-126.	0.9	3
18	Selective recovery of heavy rare earth elements from apatite with an adsorbent bearing immobilized tridentate amido ligands. Separation and Purification Technology, 2016, 159, 157-160.	7.9	37

Υοςηιακι Κον

#	Article	IF	CITATIONS
19	Fractionation of rare-earth elements during magmatic differentiation and weathering of calc-alkaline granites in southern Myanmar. Mineralogical Magazine, 2016, 80, 77-102.	1.4	27
20	Flotation of rare earth minerals from silicate–hematite ore using tall oil fatty acid collector. Minerals Engineering, 2016, 89, 52-62.	4.3	34
21	Analytical Capabilities of Elemental Imaging Using Laser Ablation-ICP-Mass Spectrometry. Journal of the Mass Spectrometry Society of Japan, 2015, 63, 153-158.	0.1	2
22	Spatial U–Pb age distribution of plutonic rocks in the central Abukuma Plateau, northeastern Japan Arc. Journal of Mineralogical and Petrological Sciences, 2015, 110, 145-149.	0.9	10
23	Influence of phosphate on mobility and adsorption of REEs during weathering of granites in Thailand. Journal of Asian Earth Sciences, 2015, 111, 14-30.	2.3	44
24	Determination of 10 major and 34 trace elements in 34 GSJ geochemical reference samples using femtosecond laser ablation ICP-MS. Geochemical Journal, 2015, 49, 351-375.	1.0	17
25	Geochemical Characteristics of Apatite in Heavy <scp>REE</scp> â€rich Deepâ€Sea Mud from <scp>M</scp> inamiâ€ <scp>T</scp> orishima Area, Southeastern <scp>J</scp> apan. Resource Geology, 2014, 64, 47-57.	0.8	89
26	The formation of rodingite in the <scp>N</scp> agasaki metamorphic rocks at <scp>N</scp> omo <scp>P</scp> eninsula, <scp>K</scp> yushu, <scp>J</scp> apan – <scp>Z</scp> ircon <scp>U</scp> – <scp>P</scp> b and <scp>H</scp> f isotopes and trace element evidence. Island Arc, 2014, 23, 281-298.	1.1	17
27	Zircon U–Pb dating from the mafic enclaves in the Tanzawa Tonalitic Pluton, Japan: Implications for arc history and formation age of the lower-crust. Lithos, 2014, 196-197, 301-320.	1.4	14
28	In-situ analyses of phosphorus contents of carbonate minerals: Reconstruction of phosphorus contents of seawater from the Ediacaran to early Cambrian. Gondwana Research, 2014, 25, 1090-1107.	6.0	27
29	Geochemical and mineralogical characteristics of ion-adsorption type REE mineralization in Phuket, Thailand. Mineralium Deposita, 2013, 48, 437-451.	4.1	116
30	Recycled crustal zircons from podiform chromitites in the <scp>L</scp> uobusa ophiolite, southern <scp>T</scp> ibet. Island Arc, 2013, 22, 89-103.	1.1	82
31	U–Pb ages of detrital zircons within the Inthanon Zone of the Paleo-Tethyan subduction zone, northern Thailand: New constraints on accretionary age and arc activity. Journal of Asian Earth Sciences, 2013, 74, 50-61.	2.3	27
32	Provenance and origins of a Late Paleozoic accretionary complex within the Khangai–Khentei belt in the Central Asian Orogenic Belt, central Mongolia. Journal of Asian Earth Sciences, 2013, 75, 141-157.	2.3	24
33	Formation Process of Zircon Associated with <scp>REE</scp> â€Fluorocarbonate and Niobium Minerals in the <scp>N</scp> echalacho <scp>REE</scp> Deposit, <scp>T</scp> hor <scp>L</scp> ake, <scp>C</scp> anada. Resource Geology, 2013, 63, 1-26.	0.8	10
34	Petrogenesis of the ridge subduction-related granitoids from the Taitao Peninsula, Chile Triple Junction Area. Geochemical Journal, 2013, 47, 167-183.	1.0	15
35	Geochemical characteristics determinedby multiple extraction from ion-adsorption type REE ores. Bulletin of the Geological Survey of Japan, 2013, 64, 313-330.	0.7	18
36	Characteristics of zircon suitable for REE extraction. International Journal of Mineral Processing, 2012, 102-103, 130-135.	2.6	9

Υοςηιακί Κον

#	Article	IF	CITATIONS
37	Detrital zircons from the Tananao metamorphic complex of Taiwan: Implications for sediment provenance and Mesozoic tectonics. Tectonophysics, 2012, 541-543, 31-42.	2.2	52
38	U-Pb zircon ages of Abukuma granitic rocks in the western Abukuma plateau, northeastern Japan Arc. Journal of Mineralogical and Petrological Sciences, 2012, 107, 183-191.	0.9	20
39	Evaluation of Laser Ablation in Liquid (LAL) technique as a new sampling technique for elemental and isotopic analysis using ICP-mass spectrometry. Journal of Analytical Atomic Spectrometry, 2011, 26, 1393.	3.0	23
40	Determinations of Rare Earth Element Abundance and U-Pb Age of Zircons Using Multispot Laser Ablation-Inductively Coupled Plasma Mass Spectrometry. Analytical Chemistry, 2011, 83, 8892-8899.	6.5	85
41	The development of whole rock analysis of major and trace elements in XRF glass beads by fsLA-ICPMS in GSJ geochemical reference samples. Geochemical Journal, 2011, 45, 387-416.	1.0	23
42	LA ICP MS U–Pb ages of detrital zircons from Russia largest rivers: Implications for major granitoid events in Eurasia and global episodes of supercontinent formation. Journal of Geodynamics, 2010, 50, 134-153.	1.6	80
43	Laser ablation ICP mass spectrometry for zircon U–Pb geochronology of ultrahigh-temperature gneisses and A-type granites from the Achankovil Suture Zone, southern India. Journal of Geodynamics, 2010, 50, 286-299.	1.6	29
44	Grain-scale iron isotopic distribution of pyrite from Precambrian shallow marine carbonate revealed by a femtosecond laser ablation multicollector ICP-MS technique: Possible proxy for the redox state of ancient seawater. Geochimica Et Cosmochimica Acta, 2010, 74, 2760-2778.	3.9	59
45	Are the Taitao granites formed due to subduction of the Chile ridge?. Lithos, 2009, 113, 246-258.	1.4	46
46	Detrital zircon evidence for the antiquity of Taiwan. Geosciences Journal, 2009, 13, 233-243.	1.2	20
47	Reworking of Hadean crust in the Acasta gneisses, northwestern Canada: Evidence from in-situ Lu–Hf isotope analysis of zircon. Chemical Geology, 2009, 259, 230-239.	3.3	117
48	Retrogressed eclogite (20kbar, 1020°C) from the Neoproterozoic Palghat–Cauvery suture zone, southern India. Precambrian Research, 2009, 171, 23-36.	2.7	93
49	Stability of pargasite during ultrahigh-temperature metamorphism: A consequence of titanium and REE partitioning?. American Mineralogist, 2009, 94, 535-545.	1.9	22
50	The youngest blueschist belt in SW Japan: implication for the exhumation of the Cretaceous Sanbagawa highâ€ <i>P/T</i> metamorphic belt. Journal of Metamorphic Geology, 2008, 26, 583-602.	3.4	63
51	Internal structures and U–Pb ages of zircons from a tuff layer in the Meishucunian formation, Yunnan Province, South China. Gondwana Research, 2008, 14, 148-158.	6.0	45
52	The Grenvillian and Pan-African orogens: World's largest orogenies through geologic time, and their implications on the origin of superplume. Gondwana Research, 2008, 14, 51-72.	6.0	377
53	Evaluation of the Analytical Capability of NIR Femtosecond Laser Ablation-Inductively Coupled Plasma Mass Spectrometry. Analytical Sciences, 2008, 24, 345-353.	1.6	67
54	Progressive metamorphism of the Taitao ophiolite; evidence for axial and off-axis hydrothermal alterations. Lithos, 2007, 98, 233-260.	1.4	21